Letters in Applied NanoBioScience
Open-Access Journal (ISSN: 2284-6808)

Article
Volume 13, Issue 4, 2024, 170
https://doi.org/10.33263/LIANBS134.170

Facile Synthesis of Copper Oxide Micro/-Nanostructures with Prospective Insecticidal Activity on Fall Armyworm (*Spodoptera frugiperda*)

Haytham A. Ayoub [1,2,*], Mohamed Khairy [1], Hosam Mohamed Khlil Hammam El-Gepaly [2]

1. Chemistry Department, Faculty of Science, Sohag University, Sohag, 82524, Egypt
2. Plant Protection Research Institute, Agricultural Research Center, Giza,12618, Egypt

* Correspondence: drayouby2020@gmail.com;

Scopus Author ID 57199646431

Received: 11.09.2023; Accepted: 11.05.2024; Published: 25.08.2024

Abstract: Nanotechnology provides innovative agrochemicals for improving crop production and quality by fabricating nanomaterial-based agrochemicals (i.e., nano-pesticides). The application of nano-pesticides in modern agriculture offers efficient programs for pest management. Herein, Copper oxide with flower-like structure (CuO-FLS) and rod-like structure (CuO-RLS) were synthesized via simple wet chemical methods and applied against Fall Armyworm (Spodoptera Frugiperda). The synthesized copper oxide micro/-nanostructures were characterized by wide-angle powder X-ray diffraction (XRD), Fourier transform-infrared (FT-IR), N_2 adsorption/desorption isotherms to determine surface properties, and Field-emission scanning electron microscopy (FE-SEM) to investigate the morphology. XRD and FT-IR analysis confirms the formation of highly crystalline materials of the monoclinic Tenorite CuO. Surface measurements showed that CuO-NPs revealed type IV isotherm with specific surface areas of SBET = 40.54 and 52.63 m^2/g for CuO-FLS and CuO-RLS, respectively. FE-SEM illustrates the formation of aggregated needles with an average diameter of 100-200 nm arranged in a hierarchical flower-like structure with an average size of 1.0 µm (CuO-FLS) and rod-like microstructure with an average size of 0.5-1.0 µm (CuO-RLS). The physicochemical properties of the synthesized CuO have a role in their insecticidal activity. The insecticidal activity for both is comparable without signifying differences between mortalities. CuO-FLS has a higher insecticidal effect (LC50=118.68 ppm) than CuO-RLS (LC50 = 134.95 ppm).

Keywords: metal oxide nanostructures; copper oxide nanoparticles; nano-pesticides; Spodoptera frugiperda.

1. Introduction

Nanomaterials provide promising alternatives to modern agriculture. Thus, applying nanomaterial-based agrochemicals (nano-fertilizers and nano-pesticides) instead of conventional ones paves the way for sustainably improving crop productivity [1-3]. In this context, synthesizing metal-oxide nanostructures attracted much attention due to their fascinating novel properties, which can be applied in engineering, industry, medicine, and agriculture [4, 5]. Copper oxide nanoparticles (CuO-NPs) are among the most widely applied transition metal oxides. CuO-NPs have a narrow band gap (~2.0 eV) with a distinct good electrochemical activity, high specific surface area, proper redox potential, and excellent stability in solutions [6, 7].

Utilizing CuO-NPs (≈50 nm) enhanced seed germination and root growth of demonstrated soybean and chickpea. Such enhancement was concentration-dependent; CuO-NPs enhanced seed germination up to 2000 ppm while root growth was prevented only at 500 ppm concentration [8]. *Penicillium* fungi create the most important disease of citrus fruits (Green Mold, Blue Mold), and the antifungal properties of synthesized CuO-NPs were tested against Penicillium on orange fruit using the disc diffusion method. The results stated that CuO-NPs antifungal activity increased by increasing the concentration to15% [9]. *Khanderao Pagar et al.* used *Moringa oleifera* leaf extract to synthesize CuO-NPs *via* a simple green chemical approach. The synthesized CuO-NPs showed potential antifungal activity against *Candida albicans*, *Aspergillus niger*, *Aspergillus clavatus*, *Trichophyton mentagrophytes*, and *Epidermophyton floccosum* [10]. The co-precipitation method was utilized to prepare CuO-NPs to apply in the management of cotton leafworm (*Spodoptera littorals*), which attack all crops and vegetables. The results showed potent entomotoxic effects (LC_{50}= 62.5 ppm for 2nd instar, LC_{50}= 300 ppm for 4th instar) besides a significant impact on the biological features of the treated insects, our previous study confirms the acute (fast entomotoxic) effect of CuO-NPs on cotton leafworm (*Spodoptera littorals*) with LC_{50} = 232.75 ppm after only three days [11, 12].

Fall Armyworm, *Spodoptera frugiperda* (Lepidoptera: Noctuidae), is a polyphagous insect pest attacking a wide range of agricultural host plants, including maize, cotton, rice, soybean, sorghum, millet, sugarcane, and many kinds of grasses [13]. Synthetic insecticides are currently considered the principal control strategy for this dangerous pest [14]. Therefore, in this study, copper oxide micro/-nanostructures (Flower-like, CuO-FLS, and Rod-like, CuO-RLS) were synthesized *via* simple wet chemical methods, and their prospective activity as alternative insecticides on Fall Armyworm (*Spodoptera frugiperda*) have been evaluated.

2. Materials and Methods

2.1. Chemicals.

All chemicals were of the highest analytical grades from Sigma-Aldrich Ltd. And used as received without further purification. Copper acetate monohydrate ($Cu(CH_3COO)_2.H_2O$), Citric acid, Ammonium hydroxide (NH_4OH, 28%), Sodium hydroxide (NaOH). Aqueous solutions were freshly prepared using bi-distilled water with resistivity > 18.2 MΩ/cm at 25°C.

2.2. Synthesis of CuO with flower-like structure (CuO-FLS).

The direct precipitation method has been used to synthesize copper oxide nanostructures with flower-like structures [12]. In typical synthesis, 0.1 mol/L (50 mL) of $Cu(CH_3COO)_2.H_2O$ was prepared in 250 mL beaker, the $Cu(CH_3COO)_2$ solution was heated and maintained under magnetic stirring at 60°C, then addition of ammonia solution (28%) dropwise till the appearance of pale blue color of $[Cu(NH_3)_6]^{2-}$, excess amount of ammonia solution was added to dissolve the formed complex. Finally, a solution of 0.1 mol/L of NaOH was added dropwise until the black precipitate of CuO was formed. The beaker mixture was left to cool. The precipitate was filtrated and dried at 60°C (Scheme 1).

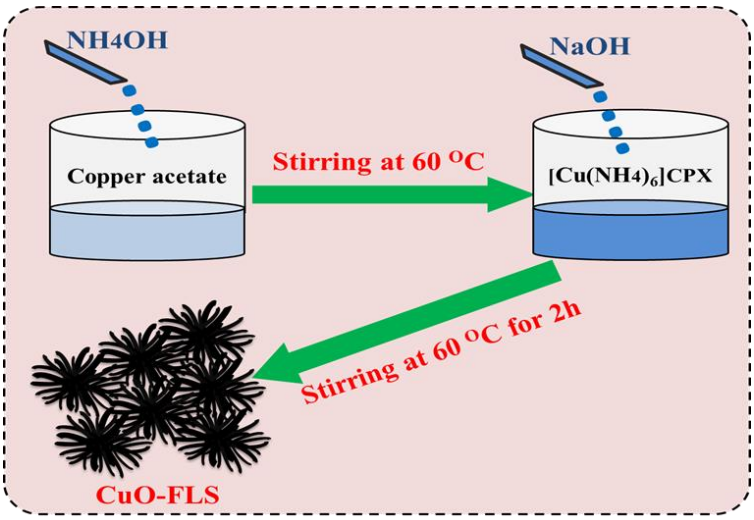

Scheme 1. Synthesis steps of copper oxide with flower-like structure (CuO-FLS) *via* direct precipitation method.

2.3. Synthesis of CuO with rod-like structure (CuO-RLS).

Sol-Gel method has been used to synthesize copper oxide nanostructures with rod-like structures [12]. In a typical synthesis, 1.0 g of citric acid was dissolved in 50 mL of distilled water, and the solution was maintained under magnetic stirring at 100°C for 15 min. A 50 mL of 0.2 mol/L Cu $(CH_3COO)_2$ was introduced dropwise to the citric acid solution, followed by ammonia solution (28%) until a black precipitate was formed. The precipitate was filtrated, washed several times with ethanol/water mixture, and dried at 60°C overnight (Scheme 2).

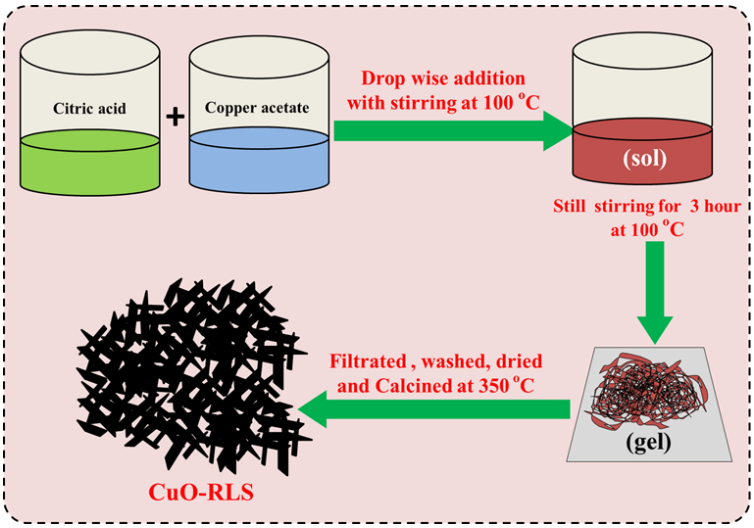

Scheme 2. Synthesis steps of copper oxide with rod-like structure (CuO-RLS) *via* sol-gel method.

2.4. Characterization of copper oxide micro/-nanostructures.

Wide-angle powder X-ray diffraction (XRD) patterns were measured; X-ray diffractometer (Model FW 1700 series, Philips, Netherlands) using monochromatic CuKα radiation (λ=1.54 Å), employing a scanning rate of 0.060 min^{-1}. The diffraction data were analyzed using PDF-2 Release 2009.

A Bruker Alpha Fourier transform-infrared (FT-IR) instrument was used to record copper oxide FT-IR spectroscopy.

Copper oxide surface properties were determined by N_2 adsorption/desorption isotherms at 73 K by using the BELSORP apparatus in Japan. Brunauer–Emmett–Teller (BET) method was utilized for calculating the specific surface area was calculated, while pore size distribution was determined from the analysis of the desorption branch of isotherm using the Barrett-Joyner-Halenda (BJH) method.

Field-emission scanning electron microscopy (FE-SEM, JEOL model 5400 LV) has been utilized to investigate the morphology of copper oxide. High-resolution images were obtained *via* operating FE-SEM at 15 kV.

2.5. Insects.

One field strain of Fall Armyworm (*Spodoptera frugiperda*) egg masses was collected from different maize fields in Sohag Governorate, Egypt. The egg masses reared for one generation under controlled laboratory conditions (Temperature 25 ± 2°C, Relative humidity 65 ± 5%, and photoperiod 8 h: 16 h, light: darkness). The leaves of the castor bean plant (*Ricinus communis L.*) were used for cultivation during the larvae stage [15].

2.6. Bioassay.

The insecticidal activity of copper oxide samples was evaluated *via* the feeding bioassay method under the recommended conditions [16]. Briefly, different concentrations were prepared (50, 100, 150, 300, 400, and 500 ppm) then equivalent sizes of castor-bean plant leaves were washed and dipped into the solutions. Polysorbate 80 surfactant (0.1%) was added to the solutions to increase the adhesion of copper oxide samples with castor-bean leaves [12]. The treated and untreated leaves were introduced into Petri dishes containing one new molting 2^{nd} instar larvae of *Spodoptera Frugiperda* with a total equal number of 20 larvae for each concentration.

2.7. Statistical analysis.

Mortality percentages (3^{rd} instar larva) were calculated after three days of treatment. Abbott's formula was utilized to correct the natural mortality [17]. The T-test statistically analyzes the comparisons between the mortalities of CuO-FLS and CuO-RLS by using SPSS 10.1 software. The value of $p < 0.05$ is considered significant for all cases. The sub-lethal (LC_{25}) and lethal (LC_{50}) concentrations were calculated by using the probit analysis program [18].

3. Results and Discussion

3.1. Characterization.

The crystal structure of synthesized copper oxide micro/-nanostructures (CuO-FLS and CuO-RLS) was investigated by wide-angle X-ray diffraction and FT-IR spectra as shown (Figure 1 and Figure 2). CuO-NPs exhibited typical diffraction peaks of the monoclinic Tenorite CuO phase (JCPDS card no. 02:1040) [19]. FT-IR spectra showed vibrational modes of the Cu–O bond; absorption peaks at 427, 477,594 cm^{-1} for CuO-FLS and 481, 526,608 cm^{-1} for CuO-RLS [19]. FT-IR spectra and the appearance of sharp peaks in the diffraction patterns of CuO-NPs confirm the formation of highly crystalline materials.

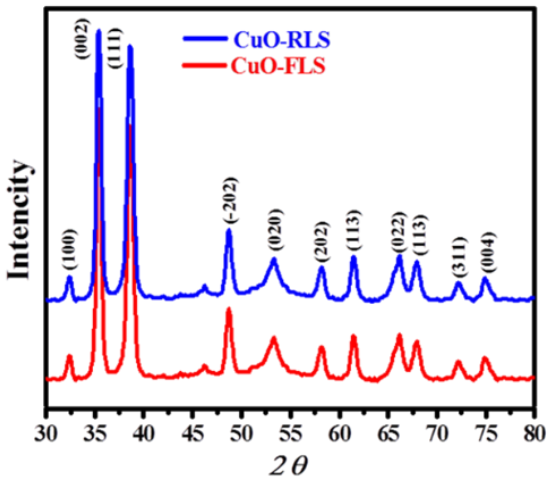

Figure 1. Wide-angle XRD of copper oxide micro/-nanostructures (CuO-FLS and CuO-RLS).

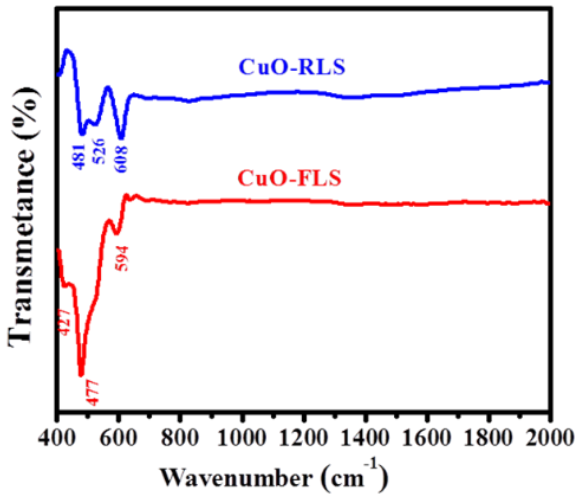

Figure 2. FT-IR of copper oxide micro/-nanostructures (CuO-FLS and CuO-RLS).

Figure 3 illustrates Nitrogen adsorption/desorption isotherms of copper oxide micro/-nanostructures (CuO-FLS and CuO-RLS). IUPAC classification showed CuO-NPs revealed a type IV isotherm with a pronounced H3 hysteresis loop, which could characterize slit-like mesopore entrances. The specific surface areas of CuO-FLS and CuO-RLS are SBET = 40.54 and 52.63 m^2/g, respectively. Copper oxide micro/-nanostructures exhibit mesoporous architectures with pore diameters of 3.38 and 12.2 nm for CuO-FLS and CuO-RLS, respectively. Interestingly, the presence of citric acid as capping increased the total surface area and pore size CuO-RLS [12].

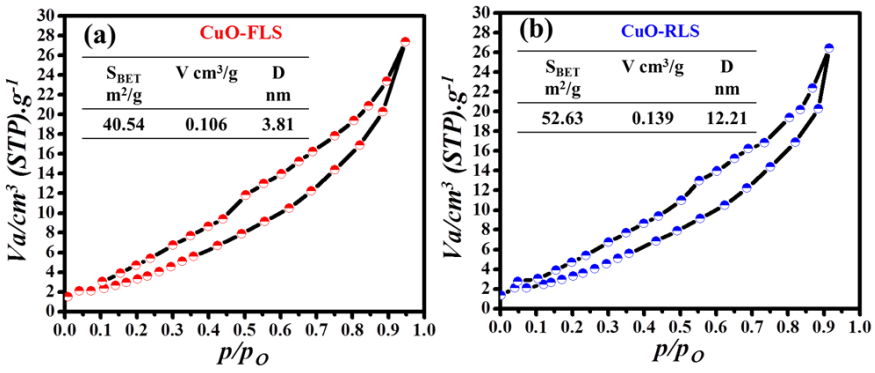

Figure 3. Nitrogen adsorption/desorption isotherms copper oxide micro/-nanostructures (CuO-FLS and CuO-RLS).

The surface morphology of copper oxide micro/-nanostructures was investigated *via* FE-SEM (Figure 4). The as-synthesized CuO-FLS is formed of aggregated needles with an average diameter of 100-200 nm arranged in a beautiful hierarchical flower-like structure with an average size of 1.0 µm (Figures 4(a,b)). Figures 4(c,d) show the formation of CuO rod-like microstructure with an average size (0.5- 1.0 µm) [12].

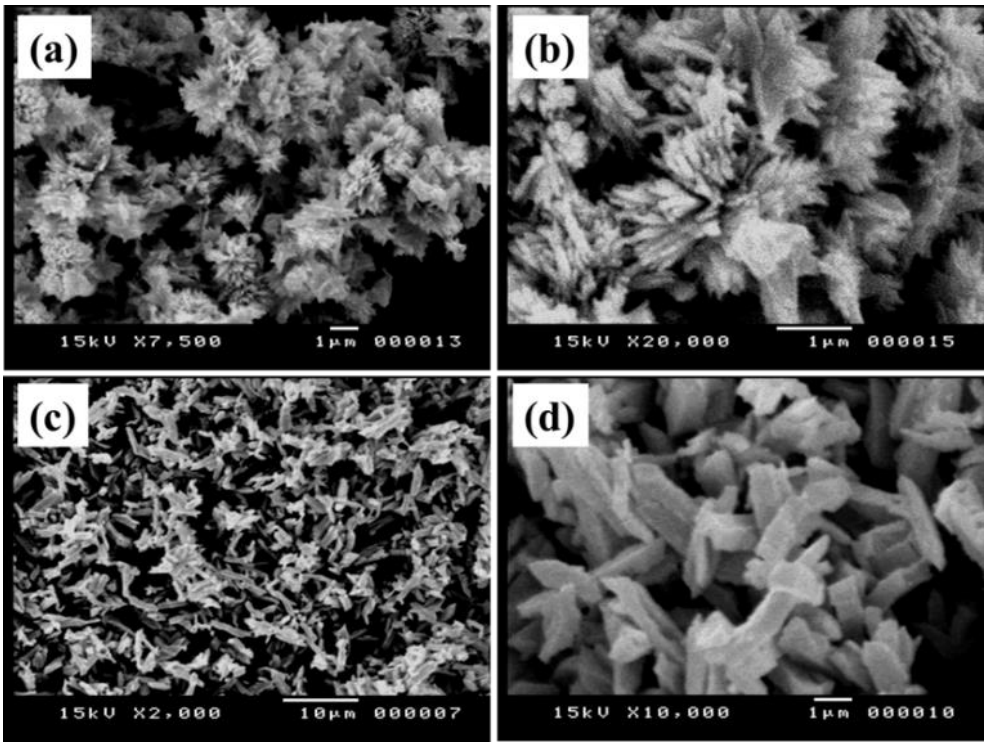

Figure 4. FE-SEM images of **(a,b)** CuO-FLS; **(c,d)** CuO-RLS.

3.2. Insecticidal activity.

The synthesized CuO-NPs produce superoxide particles in aqueous suspensions, leading to the generation of reactive oxygen radicals. These radicals stabilize as surface-bound reactive oxygen species and decay, causing damage *via* intense sorption and abrasion [20, 21]. The acute insecticidal activity of CuO-NPs against Fall Armyworm (*Spodoptera Frugiperda*) was evaluated after three days of treatment on the new molting 3rd instar larvae [17]. The mortality was concentration-dependent without signifying differences between CuO-FLS and CuO-RLS (Table 1).

Table 1. Mortality percentages of 2nd instar larvae of *Spodoptera Frugiperda* exposed to different concentrations of copper oxide micro/-nanostructures.

Concentrations (ppm)	Mortality(%) ± SD* CuO-FLS	Mortality(%) ± SD[a] CuO-RLS	df[b]	P
50	17.67 ± 1.69	13.90 ± 1.92	2	0.0129
100	41.33± 2.87	37.07 ± 2.36	2	0.1708
150	58.33 ± 2.05	55.73 ± 2.13	2	0.1499
300	83.66± 1.8	79.96 ± 1.76	2	0.0493
400	90.33± 1.72	89.83 ± 3.02	2	0.8514
500	93.33± 1.73	91.66 ± 2.06	2	0.3242

a=standard deviation; b=degree of freedom

CuO-FLS has a smaller particle size (nano-needles 100-200 nm), while the total surface area and pore size of CuO-RLS are higher than that of CuO-FLS. Thus, the insecticidal activity

for both is comparable; CuO-FLS has an LC_{50} of 118.68 ppm, and CuO-RLS has an LC_{50} of 134.95 ppm (Table 2). Therefore, particle size and surface proprieties of the synthesized copper oxide micro/-nanostructures are the key factors for their insecticidal activity [21].

Table 2. Toxicity data of 2nd instar larvae of *Spodoptera Frugiperda* exposed to different concentrations of copper oxide micro/-nanostructures.

Insecticide	(Confidence Limit at 95%)		Slope	X^2	Index	RR*
	LC_{25} (ppm)	LC_{50} (ppm)				
CuO-FLS	62.74 (55.12-70.07)	118.68 (109.32-128.03)	2.43	7.76	100	1.0
CuO-RLS	71.7698 (59.47- 83.43)	134.95 (119.61- 150.71)	2.45	4.54	88	1.13

*=resistance ratio

4. Conclusions

The application of nanomaterial-based agrochemicals provides promising alternatives for sustainably improving crop productivity. Thus, utilizing nano-pesticides instead of traditional ones may pave the way for designing efficient and applicable pest management strategies. Copper oxide with flower-like structure (CuO-FLS) and rod-like structure (CuO-RLS) were synthesized *via* simple wet chemical methods and applied as alternative insecticides for Fall Armyworm (*Spodoptera Frugiperda*) control. CuO-FLS has a smaller particle size (nano-needles 100-200 nm), while the total surface area and pore size of CuO-RLS are higher than that of CuO-FLS. Thus, the insecticidal activity is comparable without signifying differences between mortalities. CuO-FLS has a higher insecticidal effect (LC_{50}=118.68 ppm) than CuO-RLS (LC_{50} = 134.95 ppm).

Funding

Not applicable.

Acknowledgments

Not applicable.

Conflicts of Interest

The authors declare that there is no conflict of interests regarding the publication of this manuscript.

References

1. Balusamy, S.R.; Joshi, A.S.; Perumalsamy, H.; Mijakovic, I.; Singh, P. Advancing sustainable agriculture: a critical review of smart and eco-friendly nanomaterial applications. *J. Nanobiotechnology* **2023**, *21*, 372, https://doi.org/10.1186/s12951-023-02135-3.
2. Ayoub, H.A.; Khairy, M.; Rashwan, F.A.; Abdel-Hafez, H.F. Nanomaterial-based Agrochemicals New Avenue for Sustainable Agriculture: A Short Review. *J. Chem. Rev.* **2022**, *4*, 191-199, https://doi.org/10.22034/jcr.2022.336130.1163.
3. Elkady, E.F.; Ayoub, H.A.; Ibrahim, A.M. Molluscicidal activity of calcium borate nanoparticles with kodom ball-flower structure on hematological, histological and biochemical parameters of *Eobania vermiculata* snails. *Pestic. Biochem. Physiol.* **2024**, *198*, 105716, https://doi.org/10.1016/j.pestbp.2023.105716.

4. Alhalili, Z. Metal Oxides Nanoparticles: General Structural Description, Chemical, Physical, and Biological Synthesis Methods, Role in Pesticides and Heavy Metal Removal through Wastewater Treatment. *Molecules* **2023**, *28*, 3086, https://doi.org/10.3390/molecules28073086.
5. Salem, S.S.; Hammad, E.N.; Mohamed, A.A.; El-Dougdoug, W. A Comprehensive Review of Nanomaterials: Types, Synthesis, Characterization, and Applications. *Biointerface Res. Appl. Chem.* **2022**, *13*, 41, https://doi.org/10.33263/BRIAC131.041.
6. Gayathri, T.; Kumar, S.L.; Sangavi, S.; Yudhika, M.; Swathy, M. Green synthesis of copper oxide nanoparticles using Carica papaya and their antimicrobial activity. *Mater. Today: Proc.* **2023**, https://doi.org/10.1016/j.matpr.2023.11.136.
7. Khatoon, U.T.; Velidandi, A.; Rao, G.V.S.N. Copper oxide nanoparticles: Synthesis via chemical reduction, characterization, antibacterial activity, and possible mechanism involved. *Inorg. Chem. Commun.* **2023**, *149*, 110372, https://doi.org/10.1016/j.inoche.2022.110372.
8. Santos, E.S.; Graciano, D.E.; Falco, W.F.; Caires, A.R.; Arruda, E.J. Effects of copper oxide nanoparticles on germination of Sesbania virgata (FABACEAE) plants. *An. Acad. Bras. Cienc.* **2021**, *93*, e20190739, https://doi.org/10.1590/0001-3765202120190739.
9. Chalandar, H.E.; Ghorbani, H.R.; Attar, H.; Alavi, S.A. Antifungal Effect of Copper and Copper Oxide Nanoparticles Against Penicillium on Orange Fruit. *Biosci. Biotechnol. Res. Asia* **2017**, *14*, 279-284, http://dx.doi.org/10.13005/bbra/2445.
10. Pagar, K.; Ghotekar, S.; Pagar, T.; Nikam, A.; Pansambal, S.; Oza, R.; Sanap, D.; Dabhane, H. Antifungal activity of biosynthesized CuO nanoparticles using leaves extract of Moringa oleifera and their structural characterizations. *Asian J. Nanosci. Mater.* **2020**, *3*, 15-23, https://doi.org/10.26655/AJNANOMAT.2020.1.2.
11. Badawy, A.A.; Abdelfattah, N.A.H.; Salem, S.S.; Awad, M.F.; Fouda, A. Efficacy Assessment of Biosynthesized Copper Oxide Nanoparticles (CuO-NPs) on Stored Grain Insects and Their Impacts on Morphological and Physiological Traits of Wheat (*Triticum aestivum* L.) Plant. *Biology* **2021**, *10*, 233, https://doi.org/10.3390/biology10030233.
12. Ayoub, H.A.; Khairy, M.; Elsaid, S.; Rashwan, F.A.; Abdel-Hafez, H.F. Pesticidal Activity of Nanostructured Metal Oxides for Generation of Alternative Pesticide Formulations. *J. Agric. Food Chem.* **2018**, *66*, 5491-5498, https://doi.org/10.1021/acs.jafc.8b01600.
13. Kulye, M.; Mehlhorn, S.; Boaventura, D.; Godley, N.; Venkatesh, S.K.; Rudrappa, T.; Charan, T.; Rathi, D.; Nauen, R. Baseline Susceptibility of Spodoptera frugiperda Populations Collected in India towards Different Chemical Classes of Insecticides. *Insects* **2021**, *12*, 758, https://doi.org/10.3390/insects12080758.
14. Boaventura, D.; Bolzan, A.; Padovez, F.E.O.; Okuma, D.M.; Omoto, C.; Nauen, R. Detection of a ryanodine receptor target-site mutation in diamide insecticide resistant fall armyworm, *Spodoptera frugiperda*. *Pest. Manag. Sci.* **2020**, *76*, 47-54, https://doi.org/10.1002/ps.5505.
15. Ayoub, H.A.; Khairy, M.; Youssef, M.A.M. Larvicidal activity assessment for anticholinesterase insecticides against laboratory and field strains of Egyptian cotton leafworm, *Spodoptera littoralis* (Boisduval) (Lepidoptera: Noctuidae). *Zool. Entomol. Lett.* **2023**, *3*, 30-33, https://doi.org/10.22271/letters.2023.v3.i2a.69.
16. Zhu, K.Y. Insecticide Bioassay. In Encyclopedia of Entomology; Springer Netherlands, Dordrecht, **2005**; 1181–1182, https://doi.org/10.1007/0-306-48380-7_2187.
17. Abbott, W.S. A Method of Computing the Effectiveness of an Insecticide. *J. Econ. Entomol.* **1925**, *18*, 265-267, http://dx.doi.org/10.1093/jee/18.2.265a.
18. Wiegand, H. Finney, D. J.: Probit analysis. 3. Aufl. Cambridge University Press, Cambridge 1971. XV, 333 S., 41 Rechenbeispiele, 20 Diagr., 8 Tab., 231 Lit., L 5.80. *Biometrische Zeitschrift* **1972**, *14*, 72-72, https://doi.org/10.1002/bimj.19720140111.
19. Aljedaani, R.O.; Kosa, S.A.; Abdel Salam, M. Ecofriendly Green Synthesis of Copper (II) Oxide Nanoparticles Using *Corchorus olitorus* Leaves (Molokhaia) Extract and Their Application for the Environmental Remediation of Direct Violet Dye via Advanced Oxidation Process. *Molecules* **2023**, *28*, 16, https://doi.org/10.3390/molecules28010016.
20. Sajjad, H.; Sajjad, A.; Haya, R.T.; Khan, M.M.; Zia, M. Copper oxide nanoparticles: In vitro and in vivo toxicity, mechanisms of action and factors influencing their toxicology. *Comp. Biochem. Physiol. C Toxicol.Pharmacol.* **2023**, *271*, 109682, https://doi.org/10.1016/j.cbpc.2023.109682.

21. Asif, N.; Ahmad, R.; Fatima, S.; Shehzadi, S.; Siddiqui, T.; zaki, A.; Fatma, T. Toxicological assessment of Phormidium sp. derived copper oxide nanoparticles for its biomedical and environmental applications. *Sci. Rep.* **2023**, *13*, 6246, https://doi.org/10.1038/s41598-023-33360-3.